

Numerical Simulation of Axion Dynamics in the Early Universe

Joshua Lin and Zhiqian Sun

*Massachusetts Institute of Technology,
77 Massachusetts Ave., Cambridge, MA, USA*

E-mail: joshlin@mit.edu, zqsun@mit.edu

ABSTRACT: We use a 100^3 lattice to simulate QCD axions following classical equations of motion in the early universe. We consider the cosmological scenario where the Peccei-Quinn (PQ) symmetry is broken after inflation. The simulation starts before PQ symmetry breaking, then goes through QCD phase transition. To simplify the simulation, we simulate at unphysical values of the scales f_a and Λ_{QCD} , however we still observe the correct features such as axion strings and domain walls. This is the final project for Physics 212: Cosmology at Harvard University, attempting to reproduce the results in arXiv 1906.00967.

Contents

1	Theoretical Background	1
1.1	Cosmological Motivations	1
1.2	The QCD Axion	2
1.3	Radiation-dominated Universe	3
2	Computational Setup and Results	5
2.1	Initial Conditions	5
2.2	PQ-era	7
2.3	QCD era	8
3	Conclusions	9
A	Code	10

1 Theoretical Background

1.1 Cosmological Motivations

Dark matter makes up $\sim 25\%$ of the energy density of our universe, whereas ordinary matter (everything that interacts with us) makes up merely $\sim 5\%$ and the rest ($\sim 70\%$) is dark energy. Though we have an abundance of gravitational signatures of dark matter from observations such as the Bullet Cluster and Galaxy rotation curves[1], we have never had any direct detection events. We expect that dark matter, like ordinary matter, are made of particles described in some field theory. There are infinitely many different models of dark matter we can come up with, and people like to focus on the ones that solve multiple theoretical problems at once. One of such models that has gain a lot more attention in the past few decades is the QCD axion. QCD axion may make up all of dark matter in the universe, and also solves the strong CP problem in the Standard Model of particle physics.

An interesting feature of axion-like dark matter is that depending on the parameters, the resulting matter distribution can be clumped. This has implications for any experiment attempting direct detection on Earth, as we may be living in an axion-free patch of the universe. To estimate this effect, we run classical simulations of a simple axion model (complex doublet scalar), to probe the resulting mass distribution. The usually considered axion models (such as the standard DSVZ[2, 3] or KSVZ [4, 5] models) include extra degrees of freedom to attempt to explain how a light axion can exist with such small coupling to standard model matter, however they both contain a complex doublet scalar that attains (after PQ-symmetry breaking) stringy and domain-wall degrees of freedom, that we aim to simulate.

1.2 The QCD Axion

The QCD lagrangian describes physics on a large range of scales, from perturbative high-energy physics at particle colliders to low-energy physics such as confinement. Yet there is something strange - the modern perspective on ‘naturalness’ is that once we specify the symmetry and field content of a theory, we should write down all possible terms, and we expect dimensionless coefficients in such a series to be $O(1)$ numbers. In the case of QCD, such a procedure gives us:

$$\mathcal{L} = -\frac{1}{4}F_{\mu\nu}F^{\mu\nu} + \bar{\psi}_f(iD^\mu - e^{i\theta_f\gamma_5}m_f)\psi_f + \theta_1 \frac{g^2}{32\pi^2}\tilde{F}_{\mu\nu}F^{\mu\nu} \quad (1.1)$$

where f indexes the quark flavors. Note that we are free to make field redefinitions:

$$\psi_f \mapsto e^{-\frac{1}{2}i\theta_f\gamma_5}\psi'_f, \quad \bar{\psi}_f \mapsto \bar{\psi}'_f e^{-\frac{1}{2}i\theta_f\gamma_5}, \quad D\bar{\psi}D\psi \mapsto \exp\left(-i \int d^4x \theta_f \frac{g^2}{32\pi^2}\tilde{F}_{\mu\nu}F^{\mu\nu}\right) D\bar{\psi}D\psi \quad (1.2)$$

which allows us to cancel the quark phase factors, but shifts them all onto the topological-charge term. The jacobian factor can be computed in any gauge-invariant cutoff scheme, as in Fujikawa’s method, or on the lattice with Ginsparg-Wilson fermions. Note also that if we have any massless flavor of quark, we would be able to remove any θ term via field redefinitions. However the success of the quark model(/chiral perturbation theory) predictions, as well as lattice-QCD evidence seems to suggest this is not consistent with experimental data. This leaves us with the standard form of the θ -term in QCD:

$$\mathcal{L} = -\frac{1}{4}F_{\mu\nu}F^{\mu\nu} + \bar{\psi}_f(iD^\mu - m_f)\psi_f + \theta \frac{g^2}{32\pi^2}\tilde{F}_{\mu\nu}F^{\mu\nu} \quad (1.3)$$

Note that the θ -term is purely topological, and does not show up in perturbation theory. However it does have observable consequences as it is a source of CP -violation in QCD, and experimentally has been observed to be indistinguishable from zero (current experimental bounds place it at $\theta \leq 10^{-10}$). Note that the standard model as a whole is known to be CP -violating in the weak sector, so there is no symmetry reason why θ should be so close to zero. There is an industry around trying to explain this strange observation, and the axion is just one possible solution.

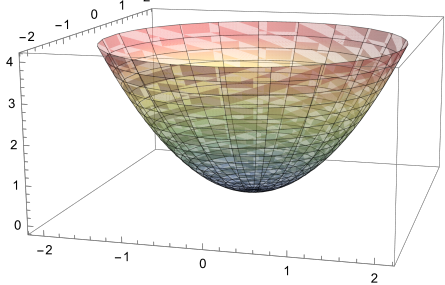
The idea behind axions is to introduce (along with additional matter fields) an additional anomalous $U(1)$ ‘Peccei-Quinn’ symmetry[6]. Just as with the $U(1)_A$ chiral anomaly in QCD, we can use this $U(1)_{PQ}$ anomaly to redefine the axion fields that would then allow us to shift all of the strong CP violation from θ_{QCD} onto the axion field. The simplest field with such a symmetry that you can write down is a complex scalar doublet:

$$\mathcal{L}_a = \frac{1}{2}|\partial_\mu\Phi|^2 - \frac{\lambda}{4}(|\Phi|^2 - f_a^2)^2 - \frac{\lambda T^2}{6}|\Phi|^2 - \frac{m_a(T)^2 f_a^2}{N^2}[1 - \cos(N\text{Arg}(\Phi))] \quad (1.4)$$

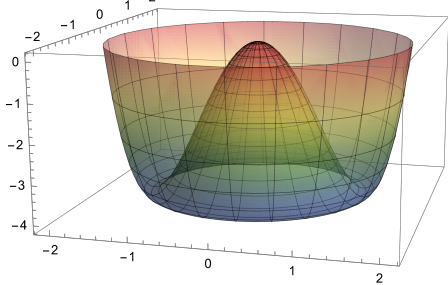
The temperature dependent axion mass models the spontaneous breaking of $U(1)_{PQ}$ by instanton effects, and has the form [7]:

$$m_a(T)^2 = \min \left[\frac{\alpha_a \Lambda^4}{f_a^2 (T/\Lambda)^n}, m_a^2 \right] \quad (1.5)$$

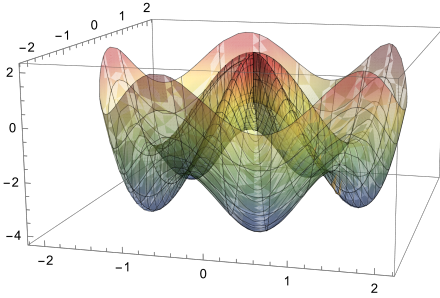
Note that there is nothing fundamental about this form, it is a fit to understand non-perturbative physics. Drawing out the potential in field space, we can get a very good understanding of the physics:



(a) Axion potential before symmetry breaking.
We initialize here, and thermal configurations
have values spread around 0.



(b) After PQ -symmetry breaking, we have
spontaneous breaking of the $U(1)$ -symmetry,
and we have vacua indexed by $U(1)$, giving us
string and domain-wall like degrees of freedom.



(c) After coupling to instantons, the symmetry
is further broken to a Z_N -subgroup. Shown
above is the potential for $N = 5$.

Figure 1: Evolution of the axion potential.

We will see in our simulations that $N > 1$ leads to long-life stable configurations of strings and domain walls, whereas $N = 1$ domain walls are unstable and evaporate after the QCD phase transition, which matches much better with current cosmological observations.

1.3 Radiation-dominated Universe

Our simulations will occur in the early radiation-dominated universe. We will review some equations, following the conventions in standard references[8]. The FLRW metric is:

$$ds^2 = dt^2 - R^2(t) \left(\frac{dr^2}{1 - kr^2} + r^2 d\Sigma^2 \right) \quad (1.6)$$

where Σ parametrises S^2 . Note that there are two different conventions for dimensions, we choose k to be dimensionless, so that $R(t)$ has dimension -1 . In what follows, we

will set $k = 0$ as a flat universe. Reminder that t here is physical time, and r refer to comoving coordinates, in other words stationary particles have fixed r , but the physical distance between such comoving particles grows. We will also later define conformal times $\eta = \frac{R}{R_1}$ for certain reference scales R_1 , depending on the era of simulation that we are in (whether we are simulating around the PQ transition or the QCD transition). Radiation dominated universe occurs when T is much larger than the mass scales of the particles (ultra-relativistic particles are effectively radiation). Some thermodynamic calculations give us:

$$p = \frac{\rho}{3}, \quad \rho = \frac{\pi^2}{30} g_* T^4, \quad g_* = N_{\text{bosons}} + \frac{7}{8} N_{\text{fermions}} \quad (1.7)$$

We have ignored complications where the different species can have different equilibrium temperatures due to decoupling. Note that g_* is a function of T , as we have various phase transitions that occur as temperature drops. We can count the particle species at different times:

$$\begin{aligned} g_*^{(T > T_{\text{EW}})} &= \frac{7}{8} \left(72_q + 12_l + 6_\nu \right) + 16_g + 2_\gamma + 9_{SU(2)} + 1_H = 106.75 \\ g_*^{(T_{\text{EW}} > T > T_{\text{QCD}})} &= \frac{7}{8} \left(60_q + 12_l + 6_\nu \right) + 16_g + 2_\gamma = 86.25 \\ g_*^{(T_{\text{QCD}} > T)} &= \frac{7}{8} \left(4_{e^\pm} + 6_\nu \right) + 2_\gamma = 10.75 \end{aligned} \quad (1.8)$$

Given that we will be simulating over these temperature ranges, it seems that we will need to keep track of the temperature dependence of g_* , but [9] claims we don't need to, and sets $g_* = 81$ as a constant, which we shall follow. We can derive some physical quantities in terms of the temperature:

$$\frac{\rho}{\rho_C} = 1 \implies H = \sqrt{\frac{4\pi^3}{45} g_*^{\frac{1}{2}} T^2 m_{\text{Planck}}^{-1}} \approx 1.660 g_*^{\frac{1}{2}} T^2 m_{\text{Planck}}^{-1} \quad (1.9)$$

$$R \propto t^{\frac{1}{2}} \implies t = \sqrt{\frac{45}{16\pi^3} g_*^{-\frac{1}{2}} T^{-2} m_{\text{Planck}}} \approx 0.3012 g_*^{-\frac{1}{2}} T^{-2} m_{\text{Planck}} \quad (1.10)$$

We have two specific temperatures of interest. The first is when $H_1^{PQ} = f_a$, the characteristic axion scale. We can derive constants at this time:

$$T_1^{PQ} = \sqrt{\frac{45 f_a}{4\pi^3} g_*^{-\frac{1}{4}}}, \quad t_1^{PQ} = \frac{1}{2f_a}, \quad \eta^{PQ} := \frac{R}{R_1^{PQ}} = \left(\frac{45}{4\pi^3 g_*} \right)^{\frac{1}{4}} \sqrt{f_a m_{\text{Pl}}} T^{-1} \quad (1.11)$$

Note that by inspecting the form of the potential, we can write down where we expect the critical phase transition to occur:

$$T_c^{PQ} = \sqrt{3} f_a, \quad \eta_c^{PQ} = \left(\frac{5}{4\pi^3 g_* f_a^2} \right)^{\frac{1}{4}} \quad (1.12)$$

In the early-QCD era, the temperature-dependent mass term gets turned on. We have new points of interest, first when $H_1^{QCD} = m_a(T_1^{QCD})$ will be our basepoint to define η_1^{QCD} :

$$T_1^{QCD} = \Lambda \left(\frac{45}{4\pi^3 g_*} \frac{m_{pl}^2}{f_a^2} \alpha_a \right)^{\frac{1}{4+n}} \quad (1.13)$$

and also the critical point where the axion mass saturates

$$T_c^{QCD} = \Lambda \left(\frac{f_a^2 m_a^2}{\alpha_a \Lambda^4} \right) \quad (1.14)$$

It may seem like there are many more scales involved, but really the introduction of Λ sets all the other scales, so you should think of the entire system as a three-scale problem, $m_{\text{pl}}, f_a, \Lambda$. The physical hierarchy is given by:

$$T_1^{PQ} > T_c^{PQ} > T_1^{QCD} > T_c^{QCD} \quad (1.15)$$

We will simulate at unphysically large f_a and Λ_{QCD} (as is often done in the literature), but we require that this hierarchy is respected.

2 Computational Setup and Results

We will simulate the equations of motion in a comoving box of lattice grid size 100^3 . The physical size of the box will vary between the different eras, and we will mention explicitly in those sections how large our boxsize is. The evolution we are attempting to perform starts right before the PQ symmetry breaking and stops after the QCD phase transition. Note that the field will enter the linear regime after QCD phase transition, and can be analytically evolved to matter-radiation equality [9].

2.1 Initial Conditions

We take a thermal distribution of the PQ complex scalar field $\phi = \phi_1 + i\phi_2$ at the initial early time well before PQ symmetry breaking, which is at $\eta = 0.0001$. We have correlation functions in k -space [7]:

$$\begin{aligned} \langle \phi_i(\vec{k}) \phi_j(\vec{k}') \rangle &= \frac{(2\pi)^3 n_k}{\omega_k} \delta(\vec{k} + \vec{k}') \delta_{ij}, \\ \langle \dot{\phi}_i(\vec{k}) \dot{\phi}_j(\vec{k}') \rangle &= (2\pi)^3 n_k \omega_k \delta(\vec{k} + \vec{k}') \delta_{ij}, \\ \langle \dot{\phi}_i(\vec{k}) \phi_j(\vec{k}') \rangle &= 0, \end{aligned} \quad (2.1)$$

where

$$n_k = \frac{1}{e^{\omega_k/T} - 1}, \quad \omega_k = \sqrt{|\vec{k}|^2 + m_{\text{eff}}^2}, \quad m_{\text{eff}}^2 = \left(\frac{T^2}{3} - f_a^2 \right). \quad (2.2)$$

Since $\phi_i(\vec{k})$ and $\dot{\phi}_i(\vec{k})$ are uncorrelated in momentum space, at each grid point on our lattice, we randomly draw the value of the field and its derivative according to a Gaussian distribution given by

$$\begin{aligned} \langle \phi_i(k) \rangle &= 0, \quad \langle |\phi_i(k)|^2 \rangle = \frac{n_k}{\omega_k} V, \\ \langle \dot{\phi}_i(k) \rangle &= 0, \quad \langle |\dot{\phi}_i(k)|^2 \rangle = n_k \omega_k V. \end{aligned} \quad (2.3)$$

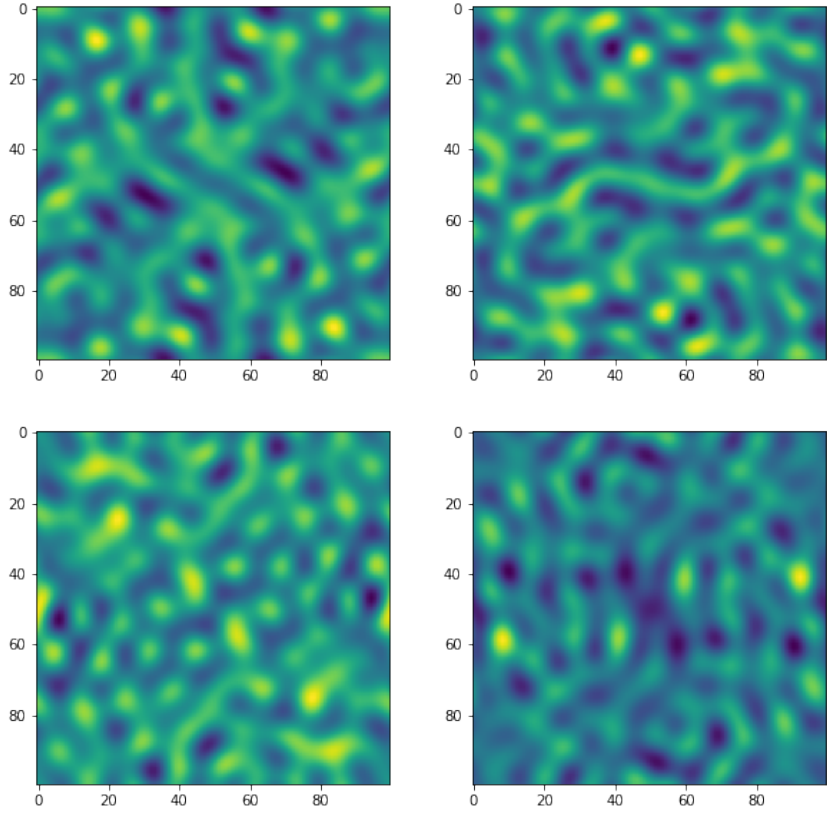


Figure 2: Sample thermal initialization of field and field derivative values on a 100^2 grid. The upper left (right) panel is ϕ_1 (ϕ_2), and the lower left (right) panel is $\dot{\phi}_1$ ($\dot{\phi}_2$).

Note that V here is the *physical* comoving volume of our simulation box and \vec{k} is the physical momentum. Explicitly, we have

$$\begin{aligned} |\vec{k}|^2 &= (k_x^2 + k_y^2 + k_z^2) \cdot (\kappa R H)^2, \\ V &= V_{\text{lat}} \cdot \left(\frac{\kappa}{R H} \right)^3. \end{aligned} \tag{2.4}$$

κ is the proportionality between the physical units and the number of lattice sites, R is the scale factor, and H is the Hubble constant. We then perform an inverse Fourier transform using `numpy.fft` to get our position space field and derivative values. In Fig. 2, we show the field and derivative values for a sample 2D initialization.

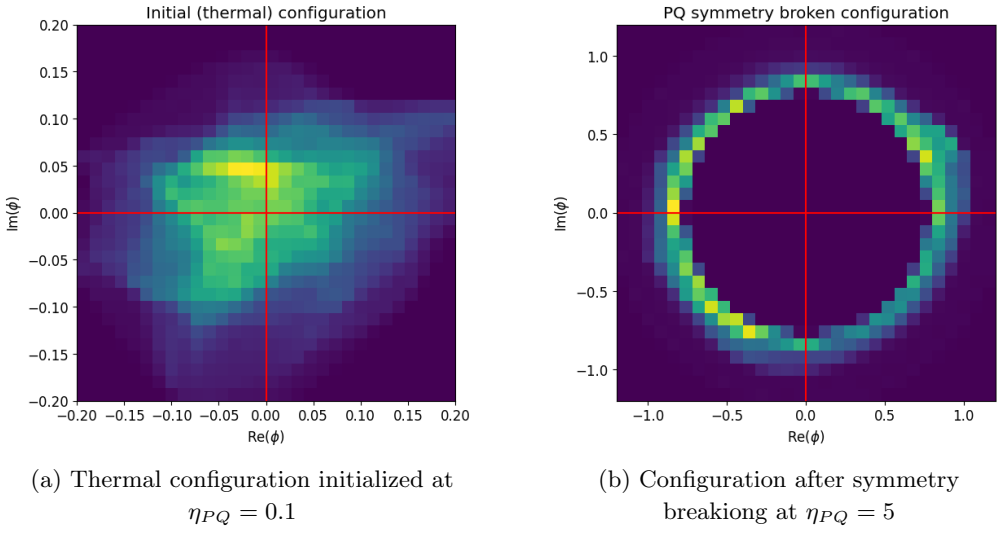


Figure 3: This figure shows histograms of the real and imaginary parts of the axion field, left is before the PQ-transition and right is after. As we can see, we dynamically break to the $U(1)$ -worth of vacua. Simulations performed on toy parameters $V = 100^3$, $f_a/m_{\text{pl}} = 0.1$ corresponding to $\eta_c^{PQ} \approx 0.47$

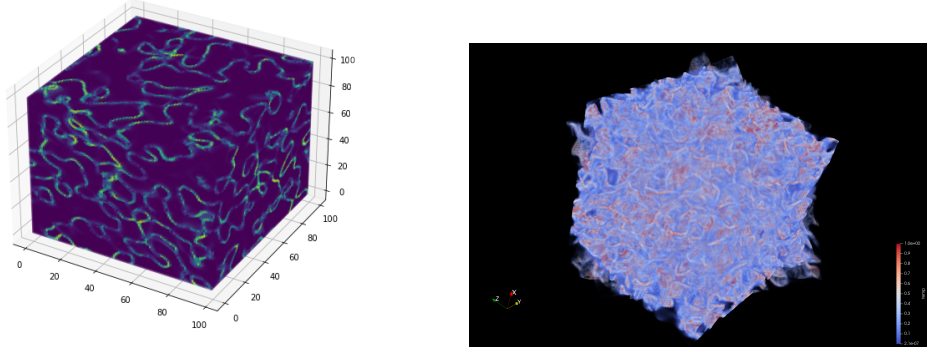
2.2 PQ-era

After initialization, we use the Runge-Kutta-Nystrom method to numerically evolve the fields according to the equations of motion until PQ symmetry breaking happening at temperature given in eq. (1.12). In the PQ-era, we assume that the temperature-dependent axion mass is negligible, and drop it from the equations of motion. This is respected as long as $f_a \gg \Lambda_{\text{QCD}}$. We will write our equations of motion in a convenient variable $\psi = \frac{\phi}{f_a \eta}$, which causes the field to be dimensionless, but also remove the damping term from the ODE:

$$\psi'' - \frac{\nabla^2}{f_a^2 R_1^2} \psi + \lambda \psi \left((|\psi|^2 - \eta^2) + \frac{T_1^2}{3 f_a^2} \right) = 0 \quad (2.5)$$

To interpret the different parameters appearing in this equation of motion, λ controls how strongly the field want to fall to the vacuum expectation value, and $\frac{T_1^2}{3 f_a^2}$ controls the critical value of η_c . As we can see in Fig. 3, the evolution dynamically generates a vacuum expectation value for the ϕ field. Axion modes are identified with the angular degrees of freedom, and before coupling to QCD are massless Nambu-Goldstone bosons. The radial modes are suppressed as temperature gets lower and lower, and eventually it is possible to remove the radial mode entirely from the simulation, though we do not do this step.

Fig. 4 show typical string and domain wall degrees of freedom after Peccei-Quinn symmetry breaking. Note that you get domain-wall like features even before breaking to QCD, where the domain-walls don't separate different vevs, but rather are just regions of large energy. (Note that in our code, the detection algorithm correctly identifies domain walls after the QCD phase transition, but the identification fails for the PQ era, i.e. they



(a) Box surface after PQ symmetry breaking (b) 3D box after PQ symmetry breaking

Figure 4: Left plot generated in matplotlib and right plot generated in Paraview.

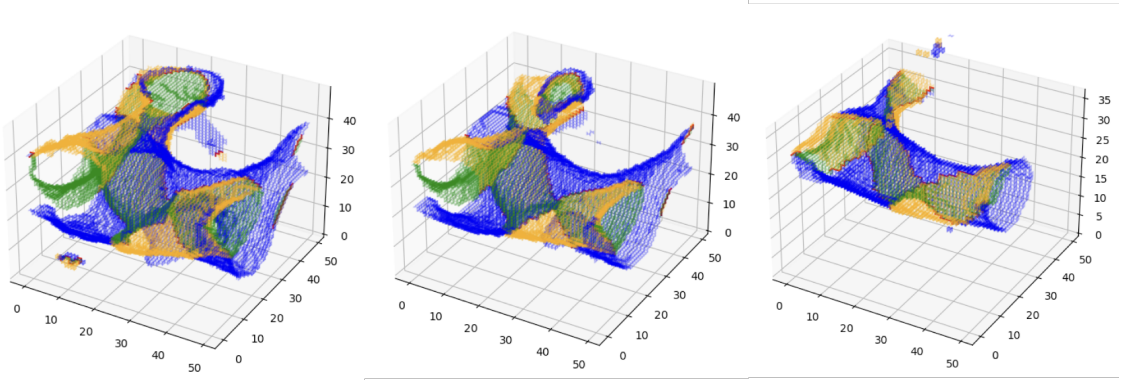


Figure 5: Simulation showing $N = 3$ before, during, and after the QCD phase transition.

would not align with large energy densities.)

2.3 QCD era

In the early QCD-era, we include the effects of the temperature-dependent mass term, but also keep all the degrees of freedom of the axion. We can make a similar change of variables as before, and we have:

$$\psi'' - \frac{\nabla^2}{f_a^2 R_1^2} \psi + \tilde{\lambda} \psi (|\psi|^2 - \eta^2) + \eta^4 \min(\eta, \eta_c)^n \frac{i\phi \sin(N \text{Arg}(\phi))}{N |\psi|^2} = 0 \quad (2.6)$$

where N is the order of the discrete Z_N subgroup that $U(1)_{PQ}$ breaks to. To identify the string and domain-wall degrees of freedom, we use a simple scheme described in [10]. Axion strings are identified by tracking field values around a plaquette and tagging the plaquette if the field values cross the real axis (in a signed way) 2 or -2 times. In the case of $N_{\text{vacua}} = 1$, the domain walls are links that are tagged by having their corresponding field values cross the negative real axis - generalizing this to higher N requires tagging links that cross half-rays that are related to the negative real-axis by roots of unity.

We simulate at $N = 1$ and $N = 3$. The string evolution at Fig. 5 show the (meta)stability of string and domain wall networks over the range of the expected QCD phase transition.

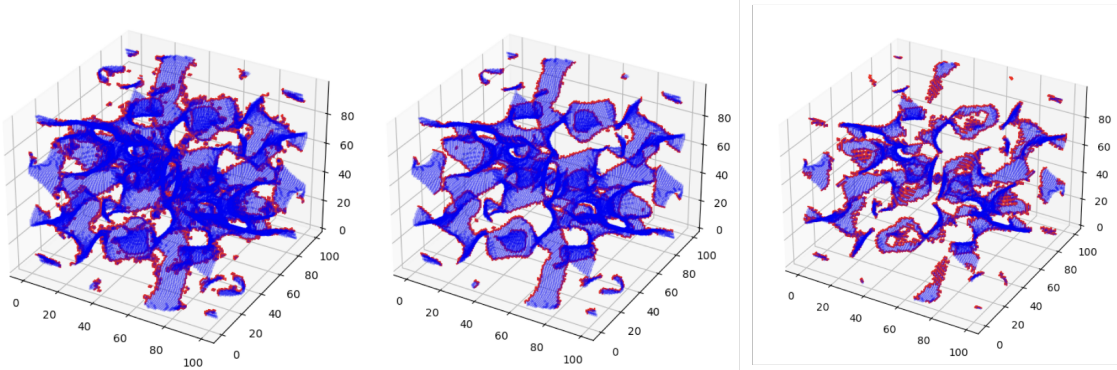


Figure 6: Simulation showing $N = 1$ before, during and after the QCD phase transition.

Note that in $N = 3$ we have three different types of domain walls (shown in orange, green, and blue) attached to strings in red. Note that we can also have ‘bubbles’ of domain walls that are not attached to any strings whatsoever, which we do observe in some runs. These (meta)stable relics are one reason why $N_{\text{vacua}} > 1$ models are highly constrained by cosmological observations, as we do not see any such relics [11].

We also simulate in Fig. 6 an $N = 1$ scenario, where we see that the strings and domain walls rapidly decay during the QCD phase transition. The resulting mass and energy density produced from the radiating strings and domain walls can then be used as phenomenological input for searches of mass overdensities in experimental data.

3 Conclusions

We’ve written code to simulate axions in a post-inflationary scenario. Our simulations have confirmed various observations from the literature, such as the (meta)stability of string and domain wall networks for $N_{\text{vacua}} > 1$, and also the existence of a scaling limit. Our code can be run as is on larger computer resources to attain larger lattice sizes (reasonably up to 512^3), anything larger would likely require actually writing MPI-code to parallelize.

There are many systematics that can be improved on (and have been explored in the existing literature). For example,

- Finite volume effects
- Finite lattice spacing artifacts
- Integration errors (oscillatory solutions make numerical integration difficult)
- Simulating far away from the physical point, in terms of $f_a, \Lambda_{\text{QCD}}$
- Time variation of g_*
- Assumption of the existence of a scaling limit after PQ-symmetry breaking
- Higher order/loop corrections to classical equations of motion

Despite this, we had a lot of fun and learnt a lot about axions and cosmology in the process. Thanks for teaching such a nice class!

A Code

We have published our code at https://github.com/joshuazlin/axion_cosmo. We include test files in the /tests folder that can regenerate the data (approximately 3GB of evolution files per run for the default parameters) and a jupyter notebook showing some of the plotting features in the /notebooks folder. We include sample data in the /notebooks

References

- [1] A. Arbey and F. Mahmoudi, *Dark matter and the early universe: A review*, *Progress in Particle and Nuclear Physics* **119** (2021) 103865.
- [2] A.R. Zhitnitsky, *On Possible Suppression of the Axion Hadron Interactions. (In Russian)*, *Sov. J. Nucl. Phys.* **31** (1980) 260.
- [3] M. Dine, W. Fischler and M. Srednicki, *A Simple Solution to the Strong CP Problem with a Harmless Axion*, *Phys. Lett. B* **104** (1981) 199.
- [4] J.E. Kim, *Weak Interaction Singlet and Strong CP Invariance*, *Phys. Rev. Lett.* **43** (1979) 103.
- [5] M.A. Shifman, A.I. Vainshtein and V.I. Zakharov, *Can Confinement Ensure Natural CP Invariance of Strong Interactions?*, *Nucl. Phys. B* **166** (1980) 493.
- [6] R.D. Peccei and H.R. Quinn, *CP Conservation in the Presence of Instantons*, *Phys. Rev. Lett.* **38** (1977) 1440.
- [7] T. Hiramatsu, M. Kawasaki, K. Saikawa and T. Sekiguchi, *Production of dark matter axions from collapse of string-wall systems*, *Phys. Rev. D* **85** (2012) 105020 [[1202.5851](#)].
- [8] E.W. Kolb and M.S. Turner, *The Early Universe*, vol. 69 (1990), [10.1201/9780429492860](#).
- [9] M. Buschmann, J.W. Foster and B.R. Safdi, *Early-Universe Simulations of the Cosmological Axion*, *Phys. Rev. Lett.* **124** (2020) 161103 [[1906.00967](#)].
- [10] L. Fleury and G.D. Moore, *Axion dark matter: strings and their cores*, *JCAP* **01** (2016) 004 [[1509.00026](#)].
- [11] D.J.E. Marsh, *Axion Cosmology*, *Phys. Rept.* **643** (2016) 1 [[1510.07633](#)].